Review

Spectrum Processing
for Quantitative Auger Electron Spectroscopy

J. T. Grant[*]
Research Institute, University of Dayton
300 College Park, Dayton OH 45469-0051, USA
[*]*j.grant@ieee.org*

There are many approaches for quantitative Auger electron spectroscopy (AES), and procedures are still being proposed. Matrix effects are usually neglected in quantitative analysis, and often result in errors by more than a factor of two. These errors arise from the neglect of electron backscattering, change in density and change in electron inelastic mean free path with change of matrix. One proposal to reduce such errors is the use of average matrix sensitivity factors instead of elemental sensitivity factors, but this approach has not yet been adopted by the AES community (and is not discussed here). This paper deals with some fundamental approaches that have been used to measure and isolate Auger peaks (and area values) for use in quantitative analysis, particularly those that were adopted in the early days of practical Auger electron spectroscopy. These early approaches include spectrum simulation, spectrum subtraction and spectrum integration, and many of their aspects are still important today.

1. Introduction

The Sixth International Vacuum Congress and the Second International Conference on Solid Surfaces was held in Kyoto, Japan, 25-29 March 1974, and it was at this meeting that I first met Prof. Keisuke Goto, to whom this special issue is dedicated. This was only a few years after the surge in interest in Auger electron spectroscopy (AES), due to the use of the lock-in amplifier to take derivatives of Auger spectra [1]. At this meeting, JEOL also introduced their first commercial Auger system, the JAMP-3. At this time, derivative Auger spectra were the norm, but the spectra were plotted on an x-y recorder. Quantitative analysis was normally accomplished by measuring peak-to-peak heights of the Auger features in a spectrum and comparing these heights with those from pure elements. The effects from electron backscattering were usually neglected, as were changes in Auger lineshapes due to chemical effects, or the use of different modulations for obtaining the derivative spectra. Laboratory or desktop computers, like we use today, were not available yet, and it was not easy to digitize the data for processing. The first digitization of Auger data that I used was accomplished using a Nicolet 1072 instrument computer in 1973 where the output from the lock-in amplifier was digitized and the data could be placed in one of four memory segments of the computer. The Nicolet instrument computer could add and subtract data from different memory locations, and could integrate and take derivatives of data. The only limitation was the number of data channels available for storing spectra, so spectra were often digitized over a limited energy range, typically 100 eV, to obtain enough data points, especially for subtraction of spectra.

At the time of the meeting in Kyoto I was researching integration methods to improve quantitative Auger analysis. This started with digital integration using the Nicolet instrument computer [2-5] and later expanded to analogue integration [6], and then to using special modulation waveforms with the lock-in amplifier to obtain integrated spectra with backgrounds removed [7,8]. Shortly thereafter, I used the Nicolet instrument computer to subtract reference spectra from Auger data to isolate overlapping components, both to retrieve accurate intensity information [9] and Auger lineshapes [10,11].

This was followed by spectrum addition to compare with measured spectra, and was done on Cu-Ni systems in collaboration with Prof. Goto who had acquired the Cu-Ni Auger spectra in his laboratory [12,13]. This work was part of a larger program to study surface segregation in Cu-Ni alloys.

This paper will discuss (1) the addition of Cu and Ni spectra to simulate spectra from Cu-Ni alloys, (2) spectrum subtraction to isolate spectra and recover Auger lineshapes, and (3) integration methods to quantify Auger intensities.

2. Experimental methods

Cu-Ni films prepared by evaporation at room temperature or above are Cu rich, and Cu is also removed preferentially with inert gas sputtering [14, 15]. Earlier studies had used the higher energy LMM Cu and Ni Auger transitions (700 – 1000 eV), and it was thought that the evaporated surfaces were homogeneous [16]. The surfaces were shown to be Cu rich by using the lower kinetic energy M_1VV transitions (80 – 120 eV) where the Auger electrons have a shorter inelastic mean free path, and are therefore a more surface sensitive measurement [14]. By controlled co-evaporation of Cu and Ni onto a liquid nitrogen cooled Ta substrate, thermal diffusion of deposited material did not occur, resulting in homogeneous compositions of the completely miscible Cu and Ni [17]. Because they are adjacent in the periodic table, no corrections for backscattering are required.

The Cu-Ni Auger spectra from the films were measured in a cylindrical mirror analyzer (CMA) using a primary beam energy of 3 keV and an analyzer modulation of 3.5 eV peak-to-peak [17]. The high energy LMM Auger peaks were used to obtain surface concentrations, and film compositions were calibrated using atomic absorption spectroscopy. The M_1VV Auger spectra were also recorded, but were not used for accurate quantification because the individual peak intensities could not be measured directly due to peak overlap. The M_1VV Cu and Ni Auger spectra used for spectrum addition, and comparison with the measured M_1VV spectra were obtained in my laboratory using a similar spectrometer and similar experimental conditions.

For spectrum subtraction, the reference spectrum was normalized to that of the spectrum being subtracted, and was very effective in isolating peaks in overlapping spectra, or in retrieving Auger lineshapes. Examples of S on Mo, Mn in steel, and CO adsorbed on metals will be used for illustration of its effectiveness.

Differentiation and integration of spectra were also accomplished in the Nicolet instrument computer. If there was a small background in the acquired derivative spectrum, it could be removed by differentiation in the instrument computer, adding or subtracting a constant from the data so the intensity on the high kinetic energy side of the Auger features could be set to zero, and then integrating. This is essentially removing a straight line background from the derivative data. At each integration step, the background on the high kinetic energy side of Auger features was set to zero. A single integration of a derivative spectrum gave the $EN(E)$ spectrum, and another integration gave the area under the peak as a function of the energy range of integration. Analog integration was accomplished by feeding the lock-in amplifier output into a single integrator, or into a double analog integrator [6]. Special waveforms (tailored modulation) were also used to modulate the outer cylinder of the CMA, resulting in $EN(E)$ type spectra or even peak areas measured for a specific kinetic energy range over the peaks of interest. Tailored modulation works for simple spectra, but does not work for spectra having many peaks over wide energy ranges [7]. However it was used to automatically remove artifacts from spectra in sputter depth profiles, and will be illustrated for silicon nitride on silicon.

3. Results and discussion

3.1. Cu-Ni alloy spectrum simulation

An example of computer simulation of Cu-Ni M_1VV spectra is shown in Fig. 1 for a 50:50 alloy where the spectra from pure Cu and pure Ni foils have been added in the instrument computer. Note that peak overlap does not allow the individual component peak-to-peak intensities to be measured accurately from Cu-Ni spectra; hence the need for a comparison of simulated spectra with the measured Cu-Ni spectra.

M_1VV Auger spectra from six Cu-Ni films are shown in Fig. 2, together with the spectra from pure Ni and Cu. The Cu/Ni atomic ratios shown in the figure were obtained from atomic absorption spectroscopy [17]. Computer simulated spectra for these atomic concentrations are shown in Fig. 3.

Note that the main M_1VV peaks correspond almost exactly to the spectra obtained from the Cu-Ni films. Spectra shown in c and d of Figs. 2 and 3 differ by only 3 at. % Cu, yet the detailed differences in peak splitting are the same for both the experimental and computer simulated spectra. Since the main features of the M_1VV spectra from all the films agree so closely with the corresponding simulated spectra, it can be concluded that the surface compositions of these films are the same as those from the bulk.
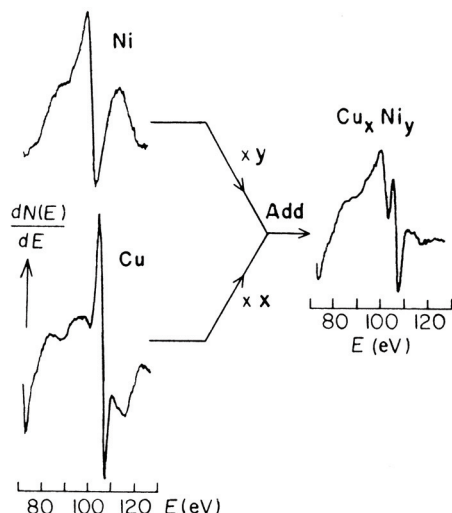
Fig. 1. Computer simulation of a Cu_xNi_y M_1VV Auger spectrum by the combination of individual Cu and Ni reference spectra (from Ref.13).
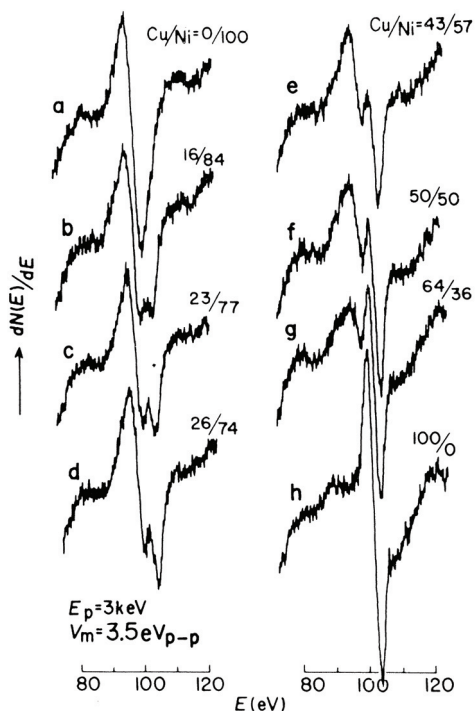

Fig. 2. Experimentally measured M_1VV Auger spectra from a series of Cu-Ni alloys (from Ref.13).
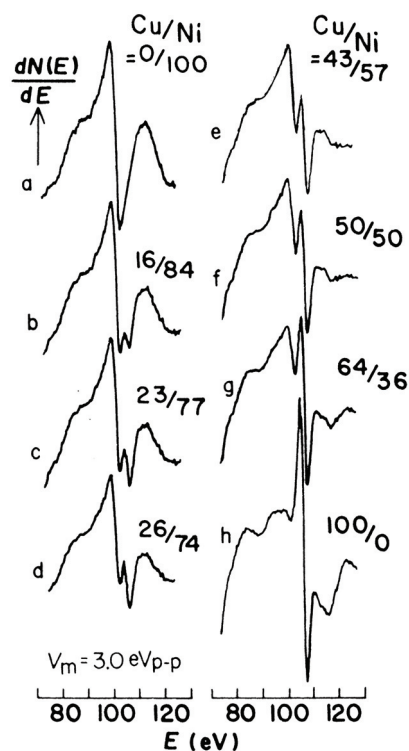

Fig. 3. Simulated M_1VV Auger spectra for a series of Cu-Ni alloys having the atomic concentrations shown, for comparison with the measured spectra in Fig. 2 (from Ref.13).

3.2. Spectrum subtraction

In AES it is easy to miss small concentrations of elements in survey spectra, particularly when peaks overlap. Two excellent examples of this are S on Mo, and Mn in low alloy steel.

The spectrum shown in Fig. 4(a) from 100 − 200 eV might look like part of the MNN spectrum from just Mo, but a careful examination of the spectrum shows that the peak near 150 eV is slightly larger than it should be for pure Mo. Typical AES spectral processing software even today does not perform such a check on all peak intensities. A reference spectrum form pure Mo is shown in Fig. 4(b), and the result (magnified by a factor of two) obtained after subtracting the reference spectrum from the measured spectrum is shown in Fig. 4(c). Note the clear isolation of the S LMM spectrum after subtraction, allowing an accurate measurement of its peak-to-peak intensity to be made [9].

An even more difficult example is shown in Fig. 5, where part of the measured spectrum from a low alloy steel sample is shown in part (b). This energy region encompasses the lowest energy peak of the main LMM Fe triplet near 595 eV and weaker Fe features at lower ki-

netic energy, as well as two peaks of the Mn LMM triplet. Amplifying the region near 540 eV by a factor of eight shows a small inflection due to Mn. The presence of this 1.4 at % Mn in the low alloy steel would go un-noticed in a normal inspection of the Auger spectrum from this sample. The result obtained after subtracting the spectrum from pure Fe (Fig. 5(a)) is shown in Fig. 5(c), at an amplification of 32 times relative to the acquired spectrum, and shows the isolated Mn Auger peak near 540 eV, the lowest energy peak of the main LMM Mn triplet (as well as another Mn peak near 585 eV, the middle peak of the main LMM Mn triplet). The intensity of this Mn peak can now be accurately measured. Note that in Fig. 5(b), the peak-to-peak height of this Auger peak would be zero due to the large background slope in this region, and that the background subtraction also removed this background [18].
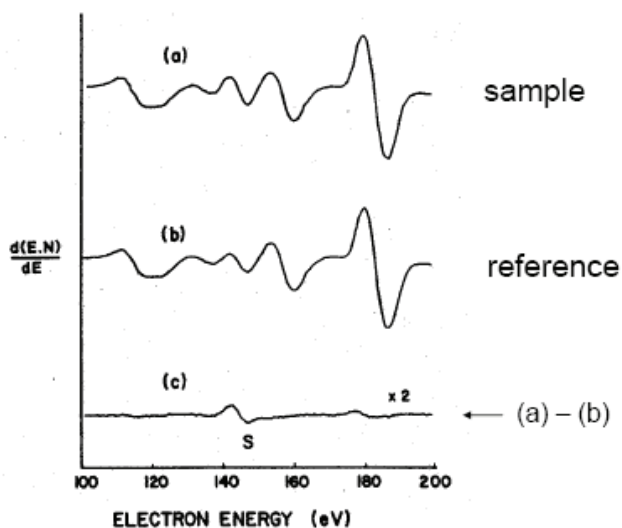
small chemical effects on the Pd lineshape [11]. The C Auger spectrum is isolated quite well however, and this C lineshape is essentially identical to the C lineshape for molecularly adsorbed CO on metals where peak overlap did not occur, such as CO on Ni [19].
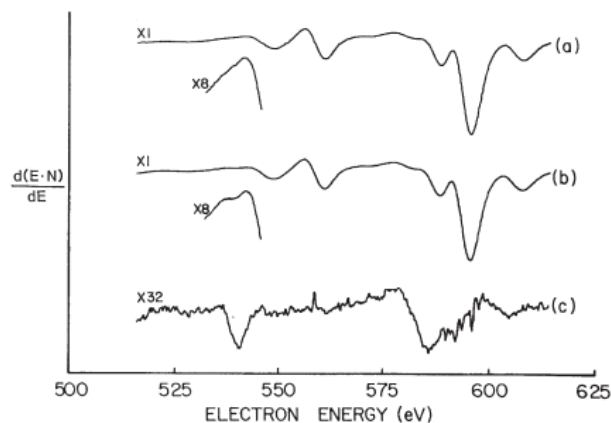

Fig. 5. Auger spectra from 515 – 615 eV from (a) pure Fe, (b) sputtered steel containing 1.4 at. % Mn, and (c) the difference spectrum at a gain of 32×.
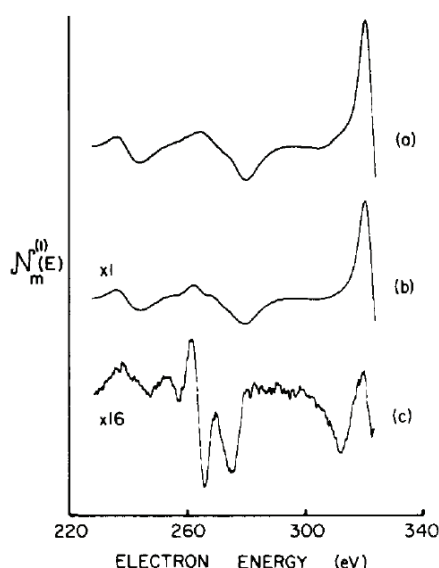

Fig. 4. Example of spectrum subtraction showing the presence of S on Mo obtained by subtracting a Mo reference spectrum from that of the sample.

Fig. 6. Auger spectra from (a) clean Pd, (b) from CO on Pd, and (c) after subtracting to retrieve the C Auger lineshape (from Ref.11)

The final example of spectrum subtraction is to show how Auger lineshapes can be retrieved from overlapping spectra. Fig. 6(a) shows part of the MNN spectrum from pure Pd, and part b shows the spectrum following CO adsorption. Note the very small change in the Auger lineshape of this spectrum in the vicinity of the C KVV Auger region, 240 – 280 eV. The difference spectrum is shown in Fig. 6(c) at 16 times amplification; note the retrieval of the C KVV Auger spectrum. The higher energy Pd signal has not been removed completely due to

3.3. Integration methods

Integration methods include digital integration, analog integration, and tailored modulation methods. All methods have been shown to be useful, but analog integration and tailored modulation never received widespread us-

age.

An early example of digital integration is shown in Fig. 7 for Ti and TiO Auger spectra. The Ti Auger lineshapes are very different and peak-to-peak heights of the Auger peaks cannot be used for quantitative analysis when such lineshape differences occur. A single integration of each derivative Auger spectrum is also shown in Fig. 7. Using peak heights from the integrated spectra reduces the error in quantitative analysis, but a further integration to measure the peak areas is needed to obtain accurate Auger signal intensities. These area values provided excellent results for main Ti Auger peaks as well as for the complete Ti Auger spectrum [2]. Note that in this early work, backgrounds were not subtracted within the Auger peak regions, and that the background was just set to zero on the high energy side of a peak before each integration was made.
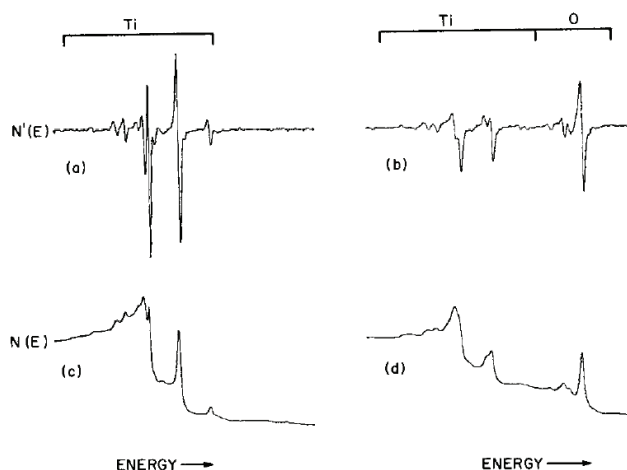

Fig. 7. (a) and (b) are derivative Auger spectra from Ti and TiO, respectively, taken with the same experimental conditions; (c) and (d) are the corresponding spectra obtained after one integration (from Ref.2).

Such simple digital integration was also shown to be useful for (a) quantification of oxygen on Ni where subtle changes in oxygen Auger lineshape could produce errors of a factor of two for oxygen concentration using peak-to-peak heights [20], and (b) exactly correcting for modulation amplitude and modulation distortion of Auger intensities in both CMA instruments [4, 21] and in retarding field analyzers [22].

An example of analog integration is shown in Fig. 8 for CO adsorbed on Mo. The derivative O KVV Auger spectrum obtained from the output of the lock-in amplifier is shown in Fig. 8(a). This analog output was fed into two analog integrators operated in series with the result of one integration shown in Fig. 8(b), and two integrations in Fig. 8(c). This double integration gives the peak area as a function of energy from the high energy side of the Auger peaks. As for digital integration, analog integration did not allow for any background subtraction within the Auger peak region. Double analog integration was successfully applied to quantify the C to O concentration on the Mo substrate [6].
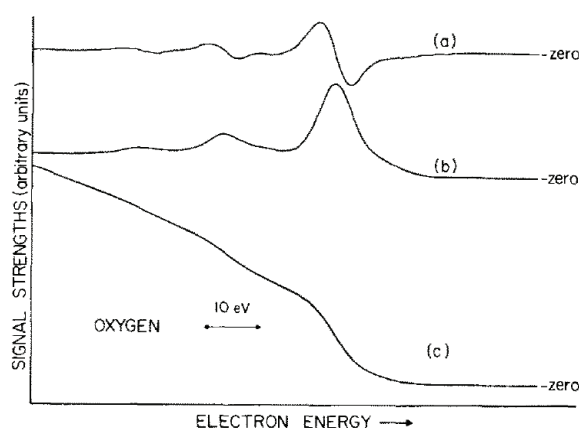

Fig. 8. Oxygen KVV spectra form CO on Mo; (a) derivative spectrum obtained from the lock-in amplifier, (b) spectrum obtained after one analog integration, and (c) result obtained after a second analog integration (from Ref.6).

Tailored modulation techniques (TMT) allow simultaneous background removal from, and peak integration of, Auger spectra. Both the order of background subtraction (first and second order), and the energy range of peak integration are chosen by selecting the modulation waveform and its amplitude [7]. An example of TMT applied to sputter depth profiling silicon nitride on silicon in a CMA system is shown in Fig. 9. The standard sputter depth profile using KLL peak-to-peak heights is plotted in Fig. 9(a), and the apparent silicon intensity decrease at the interface is due to a chemical shift between the Si KLL peak energies in silicon nitride and silicon, and not to the presence of another element at the interface [8]. This chemical shift does not allow the Auger peak-to-peak intensities to be combined correctly from the two different chemical states. Using an analyzer modulation waveform being the sum of a square wave

and a cosine wave each having peak-to-peak amplitudes of 35 eV will make the lock-in amplifier output be the Si KLL Auger peak area over an integration range of 35 eV, and the result obtained with this waveform is shown in Fig. 9b. Note that the artifact has now been removed from the sputter depth profile. TMT has also been successfully applied to sputter depth profiles of SiO_2 on Si [8] and Al_2O_3 on Al [7]. One drawback of this real time integration method was that it could not be routinely applied where there was a high degree of crowding in the spectrum as an interval above the high energy peak threshold equal to the peak width was usually required [7].
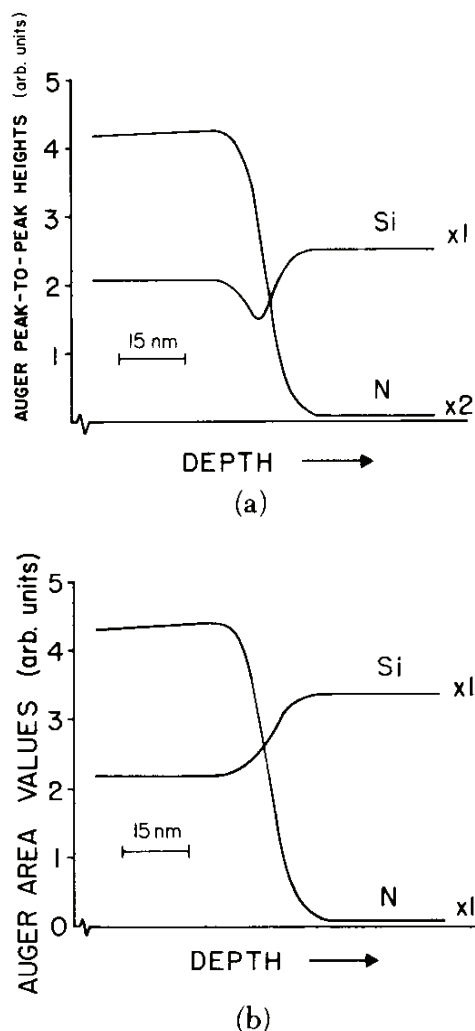

Fig. 9. Sputter depth profiles of silicon nitride on silicon, showing Auger intensities measured using (a) peak-to-peak heights of derivative spectra, and (b) Auger areas using tailored modulation (from Ref.8).

4. Summary

The several spectrum processing methods illustrated in this paper have been very useful in quantifying Auger intensities where Auger peaks overlap or where Auger lineshapes are different.

5. Dedication

This paper is dedicated to my dear friend and colleague, Prof. Keisuke Goto, and his family, on the celebration of his retirement from the Nagoya Institute of Technology. He has been a very close friend ever since I met him in March 1974, and his friendship and courtesy to my family is also very much appreciated. It is an honor to be able to contribute to this special issue.

6. References

[1] L. A. Harris, *J. Appl. Phys.* **39**, 1419 (1968).

[2] J. T. Grant, T. W. Haas, and J.E. Houston, *Phys. Letters* **45A**, 309 (1973).

[3] J. T. Grant, T. W. Haas, and J.E. Houston, *J. Vac. Sci. Technol.* **11**, 227 (1974).

[4] J. T. Grant, T. W. Haas, and J.E. Houston, *Surf. Sci.* **42**, 1 (1974).

[5] J. T. Grant, T. W. Haas and J. E. Houston, in *Proceedings of the 2nd International Conference on Solid Surfaces*, Kyoto, March 1974 (*Jpn. J. Appl. Phys. Supplement* **2**, Part 2, 1974), pp. 811-814.

[6] J. T. Grant, M. P. Hooker, and T. W. Haas, *Surf. Sci.* **46**, 672 (1974).

[7] J. T. Grant, M. P. Hooker, R. W. Springer, and T. W. Haas, *Surf. Sci.* **60**, 1 (1976).

[8] J. T. Grant, R. G. Wolfe, M. P. Hooker, R. W. Springer, and T. W. Haas, *J. Vac. Sci. Technol.* **14**, 232 (1977).

[9] J. T. Grant, M. P. Hooker, and T. W. Haas, *Surf. Sci.* **51**, 318 (1975).

[10] J. T. Grant, and M. P. Hooker, *J. Electron Spectrosc. Relat. Phenon.* **9**, 93 (1976).

[11] M. P. Hooker and J. T. Grant, *Surf. Sci.* **62**, 21 (1977).

[12] K. Goto, K. Ishikawa, R. G. Wolfe, and J.T. Grant, *Japan Society for Promotion of Science Committee for Microbeam Analysis*, No. 173, pp. 45-49 (1978). (in Japanese)

[13] K. Goto, K. Ishikawa, R. G. Wolfe, and J. T. Grant, *Appl. Surf. Sci.* **3**, 211 (1979).

[14] C. R. Helms and K. Y. Yu, *J. Vac. Sci. Technol.* **12**, 276 (1975).

[15] T. Yamashina, K. Watanabe, Y. Fukuda, and M. Ilashiba, *Surf. Sci.* **50**, 591 (1975).

[16] G. Ertl and J. Küppers, *Surf. Sci.* **24**, 104 (1971).

[17] K. Goto, T. Koshikawa, K. Ishikawa, and R. Shimizu, *J. Vac. Sci. Technol.* **15**, 1695 (1978).

[18] T. W. Haas, J. T. Grant, and M. P. Hooker, *Appl. Surf. Sci.* **2**, 433 (1979).

[19] M. P. Hooker and J. T. Grant, *Surf. Sci.* **55**, 741 (1976).

[20] M. P. Hooker, J. T. Grant, and T. W. Haas, *J. Vac. Sci. Technol.* **13**, 296 (1976).

[21] J. T. Grant, M. P. Hooker, and T. W. Haas, *J. Colloid Interface Sci.* **55**, 370 (1976).

[22] J. T. Grant and T. W. Haas, *Surf. Sci.* **44**, 617 (1974).